ECRONICON OPEN ACCESS

EC MICROBIOLOGY
Research Article

In Silico Modelling of Human Energy Metabolism

Matthew B A McCullough[1]* and Robert A Wesley[2]

[1]Chemical, Biological, and Bioengineering, North Carolina Agricultural and Technical State University, USA
[2]Department of Cardiovascular Surgery, The Miami Children's Research Institute, Miami Children's Hospital, USA

***Corresponding Author**: Matthew B A McCullough, Chemical, Biological, and Bioengineering, North Carolina Agricultural and Technical State University, USA.

Received: March 06, 2017; **Published:** March 28, 2017

Abstract

The Cori cycle (also known as Lactic acid cycle) refers to the metabolic pathway in which lactate produced by anaerobic glycolysis in the muscles moves to the liver and is converted to glucose, returns to muscle, and is metabolized back to lactate. Metabolism has been implicated in most major human diseases including obesity, diabetes, cancer, and heart disease. Understanding systemic diseases requires a fundamental and comprehensive analysis of not only the individual tissues and cell types, but also their integrated functions and interlinked interactions. Accurate physiological representation and analysis of systemic diseases however cannot be achieved unless an integrated multilevel and comprehensive modeling approach is undertaken and the appropriate computational infrastructure is fully developed and utilized. The purpose of this study was to model the complete Cori cycle of a human performing minimal activity using the pharmacokinetic/dynamic modeling software Simbiology, an add-in of Matlab. It was hypothesized that would be observed lactic acid production for a human performing minimal activity. An immediate decrease in lactic acid concentration in all tissues as well as little glycogen depletion was qualitatively assessed.

Keywords: *Cori Cycle; Simbiology; MatLab; Metabolism; Muscle*

Abbreviations

ATP: Adenosine Triphosphate; CK: Creatine Kinase

Introduction

Metabolism has been implicated in most major human diseases including obesity, diabetes, cancer, and heart disease. Thus, metabolism has been a field of study integral to many branches of medicine. In particular, obesity, a leading preventable cause of death, increases the likelihood of heart disease and diabetes, and represents one of the most serious current public health care problems. Complex examples of various metabolic interactions include the Alanine cycle, an important physiological cycle that occurs between myocytes and hepatocytes under glucose limiting conditions. The cycle's function is to eliminate nitrogen from the myocyte and transport it to the hepatocyte for degradation as urea in exchange for energy in the form of glucose. In the liver, alanine is de-aminated into Pyruvate, which serves as a substrate for gluconeogenesis. In return, glucose is supplied from the liver to skeletal muscle. In this condition, alanine was imported from the extra-system, i.e., the blood stream. The liver compartment imports alanine and produces both glucose and urea.

The Cori cycle is a metabolic cycle, similar to the Alanine cycle, which metabolically connects the peripheral tissues with the liver. Lactate acts as substrate for hepatic gluconeogenesis. As with alanine in the Alanine cycle, lactate is taken up by the liver and is converted into pyruvate, in this case by lactate dehydrogenase. Unlike the Alanine cycle, no major byproducts (e.g. urea) are generated, and thus the Cori cycle is a cycle of energy transfer between two tissues. The Cori cycle simulation involves the liver cells, muscle cells, and blood compartment. It is set up with an input of lactate into the blood from the extra-system. The Cori cycle's efficiency was validated using flux balance

analysis of the integrated multi-tissue model. The liver takes up lactate and converts it into glucose as well as gluconeogenic substrate and produces glucose for the muscle in a glucose-poor environment. The absorptive state is an anabolic process during which absorbed glucose is used by the human body to produce glycogen, triacylglycerol, and amino acids. Metabolic function of the liver during the absorptive state is closely linked to the adipose tissue and skeletal muscle for energy storage. During the absorptive state, carbohydrates and proteins in food are primarily absorbed as monosaccharides (i.e., essentially glucose) and amino acids. The liver absorbs a fraction of the blood glucose and the rest is taken up by peripheral tissues in the body to generate ATP for energy maintenance requirements. In addition to energy generation, the absorbed glucose is stored as triacylglycerol in the adipose tissue and as glycogen and proteins in the muscle tissue. The excess glucose in the liver is similarly stored as glycogen and triacylglycerol, however unlike the adipocyte, only a small amount of the synthesized triacylglycerol is stored in the liver and the rest is transported to adipose tissue.

Regular exercise or physical activity in balance, aids the human body. Exercise reduces the risk of heart disease, diabetes, and a host of other diseases, and is a significant step in healthy weight regulation. According to the 2008 Physical Activity Guidelines for Americans, regular physical activity has numerous benefits including protection from heart disease and stroke, prevention of type 2 diabetes, osteoporosis, and weight gain. It can also reduce the risk of falling and improve cognitive functions in older adults [1]. However, excessive intense physical exercise such as marathon running, crossfit, etc., can cause an athlete to develop rhabdomyolysis. Rhabdomyolysis is the breakdown of muscle tissue that leads to the release of muscle fiber contents into the blood. These substances are harmful to the kidney and often cause kidney damage. When muscle is damaged, a protein called myoglobin is released into the bloodstream. It is then filtered out of the body by the kidneys. Myoglobin breaks down into substances that can damage kidney cells [2,3]. Causes of rhabdomyolysis may include: trauma or crush injuries; use of drugs such as cocaine, amphetamines, statins, heroin, or PCP; genetic muscle diseases; extremes of body temperature; ischemia or death of muscle tissue; low phosphate levels; seizures or muscle tremors; severe exertion; and severe dehydration [2]. Symptoms include: decreased and dark, red, or cola-colored urine output; weakness, stiffness, aching, or tenderness of the affected muscles; fatigue; joint pain; Seizures; and unintentional weight gain [2]. There are medical exams which can determine if a patient is suffering from rhabdomyolysis. A physical exam will need to include the analysis of blood levels of creatine kinase (CK) level, serum calcium, serum myoglobin, serum potassium, urinalysis, and urine myoglobin. A patient will usually be administered a bicarbonate fluid intravenously, but some patients may have to undergo kidney dialysis or suffer kidney damage. Recovery for mild cases of rhabdomyolysis takes 3-4 weeks; however patients may still experience weakness or pain [2]. The severe impact of a condition like rhabdomyolysis and others would be lessened if tools that aid in the prediction of these conditions were developed. A computational model of the cori cycle would fill such a gap in the knowledge and provide useful information that contributes to better patient care.

Studying and understanding systemic diseases requires a fundamental and comprehensive analysis of the functions and interactions of cells and tissues. An accurate physiological representation and analysis of systemic diseases however cannot be achieved without an integrated multilevel and comprehensive modeling approach. This can be accomplished with the undertaking of developing an appropriate computational infrastructure [4]. Modeling the Cori cycle requires consideration of cellular and tissue scale approaches as well as the interaction between different tissues such as liver, blood, muscle, pancreas, and kidney tissue. For the Cori cycle simulations, the multi-tissue simulation finds a mass-balanced steady state by exchanging metabolites between the liver and muscle. Combining the two models had two major effects. First, since the liver and muscle became dependent on each other metabolically, the models constrained each other, shown by a lower mean flux span and higher number of fixed fluxes. A fixed flux has equivalent minimum and maximum optimized values. A multi-tissue model thus can properly simulate a physiological cycle and show intercellular interactions that an individual cell model cannot. Second, the number of fixed zero fluxes decreased in the multi-tissue simulations. The liver and muscle are linked, allowing for one cellular model to act as another's sink or source. More metabolic pathways can be potentially active in a mass balanced steady-state solution, making the multi-tissue models more robust in a nutrient limited state [4].

The purpose of this work was to create a computational kinetic model of the Cori cycle via Simbiology®, an add-in of Matlab® during minimal activity. In particular, a model of select metabolic processes, including the interactions of myoglobin, was created. It was hypothesized that minimal lactic acid production and glycogen depletion, are exhibited while a human is performing minimal activity, which is important because of the impact of Lactate on muscle tissue [5]. To study the metabolic interdependence within the human body, a novel multi-tissue modeling approach was developed to combine three cell type specific metabolic reconstructions (Figure 1) Using this preliminary model as a foundation, further research can expand the model to predict myoglobin output from the metabolic cycle. This may allow engineers and scientists to create more accurate biosensors and eliminate the need for the number of tests required when diagnosis rhabdomyolysis.

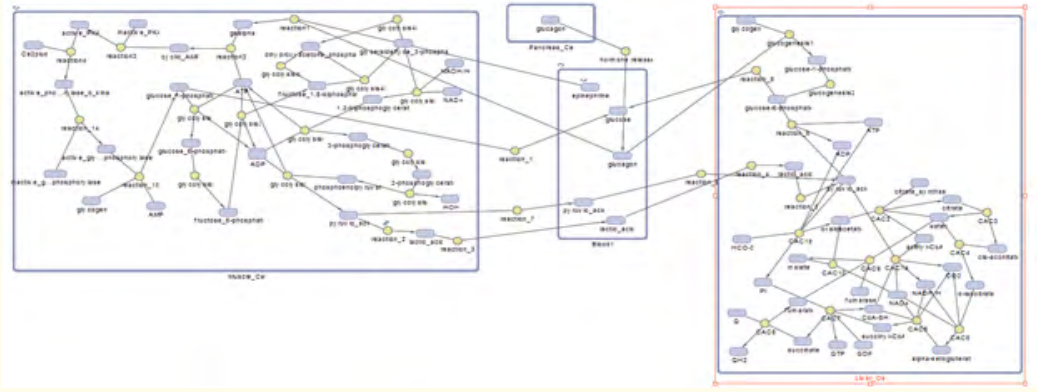

Figure 1: *Cori Cycle Model Diagram. The intermediates of glycolysis, glycogenolysis, glycogenesis, and the citric acid cycle are present.*

Materials and Methods

The method used for this research was a computational approach. Data input, creation of the model, and simulations were performed using Simbiology®, an add-in of Matlab. SimBiology® provides an app and programmatic tools to model, simulate, and analyze dynamic systems, focusing on pharmacokinetic/pharmacodynamic and systems biology applications. It provides a block diagram editor for building models, or the researcher can create models programmatically using the MATLAB® language. SimBiology® includes a library of common PK models, which can be customized and integrated with mechanistic systems biology models. SimBiology uses ordinary differential equations and stochastic solvers to simulate the time course profile of drug exposure, drug efficacy, and enzyme and metabolite levels. A researcher can investigate system dynamics and guide experimentation using parameter sweeps and sensitivity analysis. It can be used to estimate model parameters for a single subject or subject population.

This study was based on a healthy human at rest. Minimal activity being performed, perhaps in a minimal labor career. Glucagon is released from the pancreas when low levels of glycogen are detected in blood. Epinephrine initiates phosphorylation cascade in the muscle, which begins glycogenolysis, then glycolysis. From glycolysis, pyruvic acid is produced, then lactic acid. Lactic acid travels in the blood to the liver, which is converted into pyruvic acid. Pyruvic acid and acetyl-CoA are used to begin the citric acid cycle. Baseline values were considered for a fully nourished subject. Four compartments were used for this model. Liver, blood, pancreas, and muscle tissue All substrate and equilibrium constant values were assumed for aerobic conditions with the subject at rest. Undocumented initial substrate values were assumed to be equal to "0". Undocumented initial equilibrium constant values were assumed to be equal to "1". Dimensional analysis and unit conversion were performed to verify the model. All reaction rates follow the "Mass Action" and "Henri-Michaelis-Menten" principles. Initial substrate concentrations were well within human norms (Tables 1-7).

Reaction
Muscle_Cell.pyruvic_acid <-> Muscle_Cell.lactic_acid
Muscle_Cell.lactic_acid -> Blood1.lactic_acid
Blood1.lactic_acid -> Liver_Cell.lactic_acid
Liver_Cell.lactic_acid -> Liver_Cell.pyruvic_acid
Liver_Cell.pyruvic_acid + Liver_Cell.ATP -> Liver_Cell.[glucose-6-phosphate] + Liver_Cell.ADP
Liver_Cell.[glucose-6-phosphate] -> Liver_Cell.[glucose-1-phosphate]
Liver_Cell.pyruvic_acid + Liver_Cell.[CoA-SH] + Liver_Cell.[NAD+] -> Liver_Cell.[acetyl-CoA] + Liver_Cell.CO2 + Liver_Cell.[NADH/H+]
Liver_Cell.[acetyl-CoA] + Liver_Cell.oxaloacetate + Liver_Cell.water + Liver_Cell.citrate_synthase -> Liver_Cell.citrate
Liver_Cell.[glucose-6-phosphate] -> Blood1.glucose
Blood1.epinephrine + Blood1.glucagon -> Muscle_Cell.gsalpha
Muscle_Cell.gsalpha + Muscle_Cell.ATP -> Muscle_Cell.cyclic_AMP
Muscle_Cell.inactive_PKA + Muscle_Cell.cyclic_AMP -> Muscle_Cell.active_PKA
Muscle_Cell.active_PKA + Muscle_Cell.Ca2plus -> Muscle_Cell.active_phosphorylase_b_kinase
Muscle_Cell.active_phosphorylase_b_kinase + Muscle_Cell.inactive_glycogen_phosphorylase_b -> Muscle_Cell.active_glycogen_phosphorylase_a
Muscle_Cell.active_glycogen_phosphorylase_a + Muscle_Cell.AMP + Muscle_Cell.glycogen -> Muscle_Cell.[glucose_1-phosphate]
Muscle_Cell.[glucose_1-phosphate] + Muscle_Cell.ATP -> Muscle_Cell.ADP + Muscle_Cell.[glucose_6-phosphate]
Muscle_Cell.[glucose_6-phosphate] -> Muscle_Cell.[fructose_6-phosphate]
Muscle_Cell.[fructose_6-phosphate] + Muscle_Cell.ATP -> Muscle_Cell.ADP + Muscle_Cell.[fructose_1,6-biphosphate]
Muscle_Cell.[fructose_1,6-biphosphate] -> Muscle_Cell.[glyceraldehyde_3-phosphate] + Muscle_Cell.dihydroxyacetone_phosphate
Muscle_Cell.[fructose_1,6-biphosphate] -> Muscle_Cell.dihydroxyacetone_phosphate
Muscle_Cell.[glyceraldehyde_3-phosphate] -> Muscle_Cell.dihydroxyacetone_phosphate
Muscle_Cell.[glyceraldehyde_3-phosphate] + Muscle_Cell.[NAD+] -> Muscle_Cell.[NADH/H+] + Muscle_Cell.[1,3-biphosphoglycerate]
Muscle_Cell.[1,3-biphosphoglycerate] + Muscle_Cell.ADP -> Muscle_Cell.[3-phosphoglycerate] + Muscle_Cell.ATP
Muscle_Cell.[3-phosphoglycerate] -> Muscle_Cell.[2-phosphoglycerate]
Muscle_Cell.[2-phosphoglycerate] -> Muscle_Cell.HOH + Muscle_Cell.phosphoenolpyruvate
Muscle_Cell.phosphoenolpyruvate + Muscle_Cell.ADP -> Muscle_Cell.pyruvic_acid + Muscle_Cell.ATP
Liver_Cell.pyruvic_acid + Liver_Cell.[HCO-3] + Liver_Cell.ATP -> Liver_Cell.oxaloacetate + Liver_Cell.ADP + Liver_Cell.Pi
Liver_Cell.citrate -> Liver_Cell.water + Liver_Cell.[cis-aconitate]
Liver_Cell.[cis-aconitate] + Liver_Cell.water -> Liver_Cell.[d-isocitrate]
Liver_Cell.[d-isocitrate] + Liver_Cell.[NAD+] -> Liver_Cell.[NADH/H+] + Liver_Cell.CO2 + Liver_Cell.[alpha-ketogluterate]
Liver_Cell.[alpha-ketogluterate] + Liver_Cell.[NAD+] + Liver_Cell.[CoA-SH] -> Liver_Cell.[succinyl-CoA] + Liver_Cell.[NADH/H+] + Liver_Cell.CO2
Liver_Cell.[succinyl-CoA] + Liver_Cell.GDP + Liver_Cell.Pi -> Liver_Cell.[CoA-SH] + Liver_Cell.GTP + Liver_Cell.succinate
Liver_Cell.succinate + Liver_Cell.Q -> Liver_Cell.fumarate + Liver_Cell.QH2
Liver_Cell.fumarate + Liver_Cell.water + Liver_Cell.fumarase -> Liver_Cell.malate
Liver_Cell.malate + Liver_Cell.[NAD+] -> Liver_Cell.oxaloacetate
Liver_Cell.glycogen + Blood1.glucagon -> Liver_Cell.[glucose-1-phosphate]

Pancreas_Cell.glucagon -> Blood1.glucagon
Muscle_Cell.[glucose_1-phosphate] -> Blood1.glucose
Muscle_Cell.pyruvic_acid -> Blood1.pyruvic_acid
Blood1.pyruvic_acid -> Liver_Cell.pyruvic_acid

Reaction Rate	**Kinetic Law**
k1*Muscle_Cell.pyruvic_acid - [k-1]*Muscle_Cell.lactic_acid	Mass Action
k2*Muscle_Cell.lactic_acid	Mass Action
k4*Blood1.lactic_acid	Mass Action
k5*Liver_Cell.lactic_acid	Mass Action
k6*Liver_Cell.pyruvic_acid*Liver_Cell.ATP	Mass Action
[k(gluco2)]*Liver_Cell.[glucose-6-phosphate]	Mass Action
[k(cac1a)]*Liver_Cell.pyruvic_acid*Liver_Cell.[CoA-SH]*Liver_Cell.[NAD+]	Mass Action
[k(cac1)]*Liver_Cell.[acetyl-CoA]*Liver_Cell.oxaloacetate*Liver_Cell.water*Liver_Cell.citrate_synthase	Mass Action
k8*Liver_Cell.[glucose-6-phosphate]	Mass Action
[k(gsa)]*Blood1.epinephrine*Blood1.glucagon	Mass Action
[k(AMP)]*Muscle_Cell.gsalpha*Muscle_Cell.ATP	Mass Action
[k(PKA)]*Muscle_Cell.inactive_PKA*Muscle_Cell.cyclic_AMP	Mass Action
[k(active_gly_phospho_b)]*Muscle_Cell.active_PKA*Muscle_Cell.Ca2plus	Mass Action
[k(active_gly_phospho_a)]*Muscle_Cell.active_phosphorylase_b_kinase*Muscle_Cell.inactive_glycogen_phosphorylase_b	Mass Action
[k(glu_1-phos)]*Muscle_Cell.active_glycogen_phosphorylase_a*Muscle_Cell.AMP*Muscle_Cell.glycogen	Mass Action
[k(gly1)]*Muscle_Cell.[glucose_1-phosphate]*Muscle_Cell.ATP	Mass Action
[k(gly2)]*Muscle_Cell.[glucose_6-phosphate]	Mass Action
[vm(gly3)]*Muscle_Cell.[fructose_6-phosphate]/([km(gly3)]+Muscle_Cell.[fructose_6-phosphate])	Henri-Michaelis-Menten
[vm(gly4b)]*Muscle_Cell.[fructose_1,6-biphosphate]/([km(gly4b)]+Muscle_Cell.[fructose_1,6-biphosphate])	Henri-Michaelis-Menten
[vm(gly4a)]*Muscle_Cell.[fructose_1,6-biphosphate]/([km(gly4a)]+Muscle_Cell.[fructose_1,6-biphosphate])	Henri-Michaelis-Menten
[k(gly4c)]*Muscle_Cell.[glyceraldehyde_3-phosphate]	Mass Action
[k(gly5)]*Muscle_Cell.[glyceraldehyde_3-phosphate]*Muscle_Cell.[NAD+]	Mass Action
[k(gly6)]*Muscle_Cell.[1,3-biphosphoglycerate]*Muscle_Cell.ADP	Mass Action
[k(gly7)]*Muscle_Cell.[3-phosphoglycerate]	Mass Action
[k(gly8)]*Muscle_Cell.[2-phosphoglycerate]	Mass Action
[k(gly9)]*Muscle_Cell.phosphoenolpyruvate*Muscle_Cell.ADP	Mass Action
[k(cac1b)]*Liver_Cell.pyruvic_acid*Liver_Cell.[HCO-3]*Liver_Cell.ATP	Mass Action
[k(cac2)]*Liver_Cell.citrate	Mass Action
[k(cac3)]*Liver_Cell.[cis-aconitate]*Liver_Cell.water	Mass Action
[k(cac4)]*Liver_Cell.[d-isocitrate]*Liver_Cell.[NAD+]	Mass Action
[k(cac5)]*Liver_Cell.[alpha-ketogluterate]*Liver_Cell.[NAD+]*Liver_Cell.[CoA-SH]	Mass Action

[k(cac6)]*Liver_Cell.[succinyl-CoA]*Liver_Cell.GDP*Liver_Cell.Pi	Mass Action
[k(cac7)]*Liver_Cell.succinate*Liver_Cell.Q	Mass Action
[k(cac8)]*Liver_Cell.fumarate*Liver_Cell.water*Liver_Cell.fumarase	Mass Action
[k(cac9)]*Liver_Cell.malate*Liver_Cell.[NAD+]	Mass Action
[k(gluco1)]*Liver_Cell.glycogen*Blood1.glucagon	Mass Action
[k(glucagon)]*Pancreas_Cell.glucagon	Mass Action
[k(glu1phosphtoglucose)]*Muscle_Cell.[glucose_1-phosphate]	Mass Action
kpyruvic1*Muscle_Cell.pyruvic_acid	Mass Action
kpyruvic2*Blood1.pyruvic_acid	Mass Action

Table 2: *Reaction Rates.*

Parameter (Forward,Reverse)	Parameter Value (Forward,Reverse)	Units
k1,k-1	25.0, 0.04	1/second
k2	1	1/second
k4	1	1/second
k5	1	1/second
k6	0.5	1/(millimole*second)
k(gluco2)	1	1/second
k(cac1a)	1	1/((millimole^2)*second)
k(cac1)	3.75E-06	1/((millimole^3)*second)
k8	1	1/second
k(gsa)	0.5	1/(millimole*second)
k(AMP)	20	1/(millimole*second)
k(PKA)	10	1/(millimole*second)
k(active_gly_phospho_b)	100	1/(millimole*second)
k(active_gly_phospho_a)	1000	1/(millimole*second)
k(glu_1-phos)	10000	1/((millimole^2)*second)
k(gly1)	0.001739	1/(millimole*second)
k(gly2)	2.637	1/second
vm(gly3)	0.68	millimole/second
km(gly3)	4.71E-06	millimole
vm(gly4b)	1.19	millimole/second
km(gly4b)	0.045	millimole
vm(gly4a)	0.045	millimole/second
km(gly4a)	1.19	millimole
k(gly4c)	0.379	1/second
k(gly5)	32.1429	1/(millimole*second)
k(gly6)	0.003774	1/(millimole*second)
k(gly7)	0.733	1/second
k(gly8)	0.08	1/second

k(gly9)	0.002356	1/(millimole*second)
k(cac1b)	1	1/((millimole^2)*second)
k(cac2)	3.39461	1/second
k(cac3)	3.39461	1/(millimole*second)
k(cac4)	0.03842	1/(millimole*second)
k(cac5)	2.27E-06	1/((millimole^2)*second)
k(cac6)	0.32459	1/((millimole^2)*second)
k(cac7)	1	1/(millimole*second)
k(cac8)	0.228919	1/((millimole^2)*second)
k(cac9)	101064	1/(millimole*second)
k(gluco1)	1	1/(millimole*second)
k(glucagon)	1	1/second
k(glu1phosphtoglucose)	1	1/second
kpyruvic1	1	1/second
kpyruvic2	1	1/second

Table 3: *Parameters and Units.*

Muscle Tissue	
Substrate	Initial Concentration (mM)
Glycogen	4
Glucose-6-phosphate	2.45
Pyruvic acid	0.1
Lactic acid	2.5
gs alpha	0
Cyclic AMP	0
Inactive PKA	0
Active PKA	0
Ca2+	0
Active phosphorylase b kinase	0
Inactive glycogen phosphorylase b	0
Active glycogen phosphorylase a	1
AMP	2
Glucose-1-phosphate	100
Fructose-6-phosphate	6.461
ADP	1.29E-06
Fructose-1,6-phosphate	5.51E-06
Glyceraldehyde-3-phosphate	0
Dihydroxyacetone phosphate	0.81
NAD+	1.55
1,3-biphosphoglycerate	5.83E-04

NADH/H+	0.004
3-phosphoglycerate	0.52
2-phosphoglycerate	0.07
HOH	0
Phosphoenolpyruvate	0.08
ATP	2.52

Table 4: *Muscle Substrate Concentrations.*

Blood Tissue	
Substrate	Initial Concentration (mM)
Lactic Acid	1.6
Glucose	4.44
Glucagon	0.04307
Epinephrine	0.22
Pyruvic Acid	0.05

Table 5: *Blood Substrate Concentrations.*

Liver Tissue	
Substrate	Initial Concentration (mM)
Pyruvic acid	2
ATP	6
Glucose-6-phosphate	0
CoA-SH	1
CO2	1
HCO3	0
ADP	0
H2O	1
Citrate synthase	0
Citrate	0
Cis-aconitate	0
d-isocitrate	0
NADH/H+	1
Alpha-ketogluterate	0
Succinyl-CoA	0
Pi	1
GDP	0
GTP	0
Succinate	0
Q	0
Fumerate	0

QH2	0
Fumerase	0
Malate	0
Oxaloacetate	0
Acetyl-CoA	0
Glucose-1-phosphate	0
Glycogen	161.7

Table 6: *Liver Substrate Concentrations.*

Pancreas Tissue	
Substrate	Initial Concentration (mM)
Glucagon	0.04307

Table 7: *Pancreas Substrate Concentrations.*

Results and Discussion

A simulation of an adult, participating in minimal activity after eating breakfast was completed. Results from the simulation of monitored lactic acid, glucagon, epinephrine, and Pyruvic acid accumulation in the blood, over the course of five minutes are shown in Figure 2. Concentrations of epinephrine remained constant at 0.2mM/L, while concentrations of pyruvic acid were near zero for the entire simulation. Lactic acid concentration peaked at 1.8mM/L, early in the simulation (within the first 30 seconds) but were near zero by the five-minute mark (0.1mM/L).

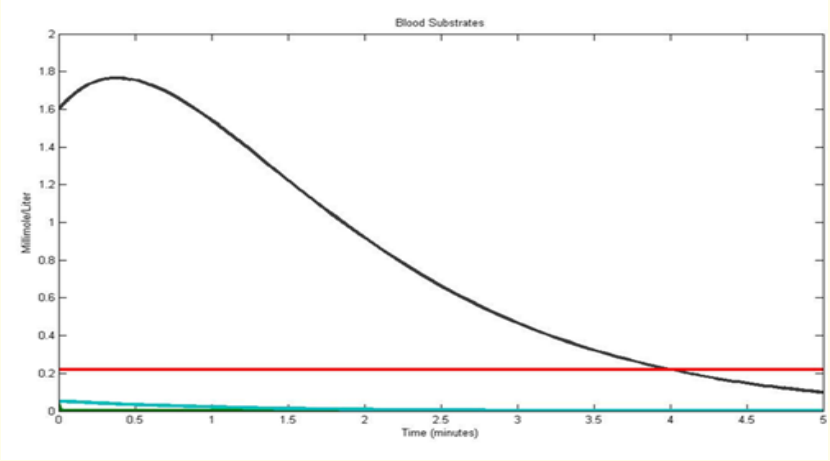

Figure 2: *Concentrations of substrates in blood over the five-minute simulation.*

Figure 3 shows the concentrations of liver substrates generally showed a decreasing trend. Lactic acid had the highest initial concentration, while ATP steadily decreased over the simulation. Glucose-6-phosphate started at zero, quickly peaked around 1mM/L after half a minute, then decreased over the course of the simulation. Pyruvic acid followed a slightly different trend, by initially decreasing, then steadily increasing over the course of the simulation.

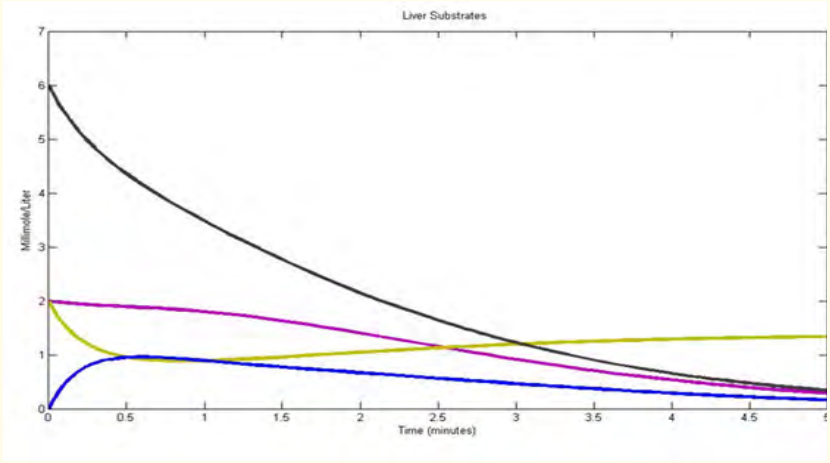

Figure 3: *Concentration of liver substrates over the five-minute simulation.*

Figure 4 shows concentrations of muscle substrates followed a general downward trend in terms of concentration over the time of simulation. Decreased concentrations were noted in Glucose-6-Phosphate, Pyruvic acid, and cell ATP. The aforementioned concentrations, except Pyruvic acid, reached zero within five minutes. Glycogen exhibited oscillatory behavior around 3 mM/L.

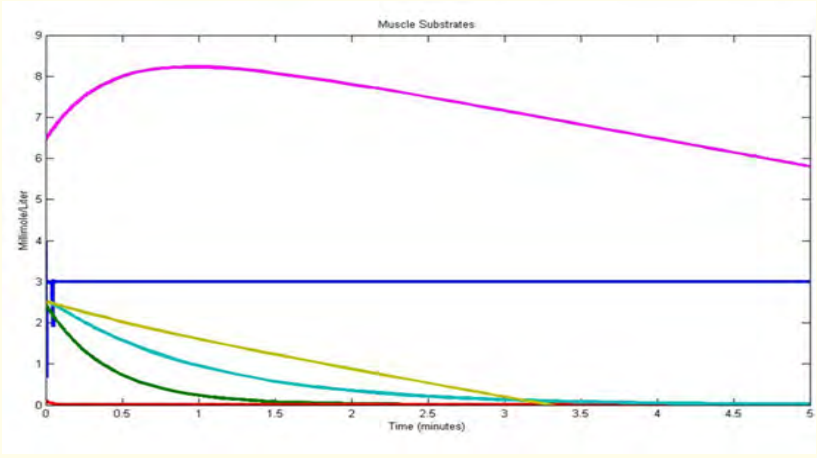

Figure 4: *Concentrations of substrates in the muscle.*

In addition to promising results, there are limitations to this model. One such limitation is the limitation of available experimental data on these reactions. Missing single compartment validation limited our ability to confirm data from the model. There were also limitations to the computational capacity of our software package. Future work could include experimental microfluidic experiments that would validate the model. And the use of supercomputing clusters may prove useful.

Conclusion

In conclusion, a preliminary model has been formulated, representing the Cori Cycle during rest. MatLab Simbiology was used to model the interactions within the metabolic cycle. A four-compartment model showed various trends in lactic acid, ATP, Pyruvic acid, Glycogyen, and Glucose-6-Phosphate.

Acknowledgements

The authors would like to acknowledge the effort and guidance of Dr. Yeoheung Yun, in the department of Chemical, Biological, and Bioengineering at North Carolina A&T State University. They would also like to acknowledge U.S. Department of Education Grant #P120A120034.

Conflict of Interest

There are no conflicts of interest to report.

Bibliography

1. Buchner DM., *et al*. "Physical Activities Guidelines for Americans" (2008).
2. Brenner BM. Brenner and Rector's the kidney (2000).
3. Nelson DL., *et al*. "Lehninger principles of biochemistry". *Macmillan* (2008).
4. Bordbar A., *et al*. "A multi-tissue type genome-scale metabolic network for analysis of whole-body systems physiology". *BMC Systems Biology* 5 (2011): 180.
5. Hogan MC and HG Welch. "Effect of varied lactate levels on bicycle ergometer performance". *Journal of Applied Physiology* 57.2 (1984): 507-513.

Volume 7 Issue 1 March 2017